NASA TECHNICAL MEMORANDUM

NASA TM-73812

NASA TM-73812

AN INTEGRATED THEORY FOR PREDICTING THE HYDROTHERMOMECHANICAL RESPONSE OF ADVANCED COMPOSITE STRUCTURAL COMPONENTS

by C. C. Chamis, R. F. Lark, and J. H. Sinclair
Lewis Research Center
Cleveland, Ohio 44135

TECHNICAL PAPER presented at the
Technical Specialists Conference "Environmental Effects on Advanced Composite Materials" sponsored by the American Society for Testing and Materials
Dayton, Ohio, September 29-30, 1977

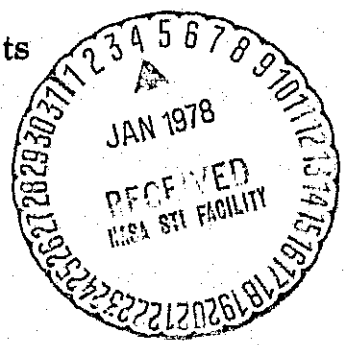

AN INTEGRATED THEORY FOR PREDICTING THE HYDRO-THERMOMECHANICAL RESPONSE OF ADVANCED COMPOSITE STRUCTURAL COMPONENTS

by C. C. Chamis,* R. F. Lark,* and J. H. Sinclair*

ABSTRACT

An integrated theory is developed for predicting the hydrothermo-mechanical (HDTM) response of fiber composite components. This integrated theory is based on a combined theoretical and experimental investigation. In addition to predicting the HDTM response of components, the theory is structured to assess the combined hydrothermal effects on the mechanical properties of unidirectional composites loaded along the material axis and off-axis, and those of angleplied laminates. The theory developed predicts values which are in good agreement with measured data at the micromechanics, macromechanics, laminate analysis and structural analysis levels.

Key Words: Composites, theory, experiment, composite mechanics, laminate theory, structural analysis, stress analysis, warpage, thermal stresses, hydro stresses, finite element analysis

*Aerospace Engineer, National Aeronautics and Space Administration, Lewis Research Center, Cleveland, Ohio 44135.

STAR Category 39

E-9372

NOMENCLATURE

(Property and direction are given by subscripts)

A	inplane stiffness array (eq. (32))
a	dimension
b	dimension
C	coupled stiffness array (eq. (32)), heat capacity
D	array of bending stiffness (eq. (32))
E	elastic modulus
F	function
$\mathcal{F}_m$	mechanical property relation (eq. (4))
$\mathcal{F}_t$	thermal property relation (eq. (5))
G	shear modulus
HDTM	abbreviation for hydrothermomechanical
K	heat conductivity
k	volume ratio
M	moment
m	moisture
$R_{\ell\epsilon}$, $R_{\ell\sigma}$	transformation matrix for strain and stress respectively
S	ply uniaxial strength
T_g	glass transition temperature
T_s	resin softening temperature = T_g
T_c	reference temperature (273 K)
w	out-of-plane displacement
x, y, z	structural axes reference coordinates
1, 2, 3	material axes reference coordinates
α	thermal expansion coefficient
β	moisture coefficient

β_v	void magnification factor
β_{sub}	correlation coefficients, taken as unity if not defined
ϵ	strain
ϵ_{co}	reference plane inplane strain (eq. (32))
θ	ply orientation angle taken positive for transformations from the old to the new axis.
κ	local curvature (eq. (32))
ν	Poisson's ratio
ρ	density
σ	stress
φ_μ	strain magnification factor
$[\ ]$	square array
$[\ ]^T$	transpose
$[\ ]^{-1}$	inverse
$\{\ \}$	column vector
$\|\ \| = \{\ \}^T$	row vector

Subscripts

C	compression
c	composite property
d	dry property
f	fiber property
g	glass transition
H	hydro (moisture) property
ℓ	ply (unidirectional) composite property
m	moisture property
r	resin property
S	shear property
T	tension
t	thermal property

v	void
w	wet property
x, y, z	property or variable referred to structural axes
o	reference temperature (T_o = 273 K) dry property
1, 2, 3	property or variable referred to material axes

INTRODUCTION

The influence of hydrothermal environments on advanced composite mechanical properties has been extensively investigated by the composites community over the past several years (refs. 1 to 5). The various investigations thus far have generated significant fundamental knowledge for: (1) identifying the variables and mechanisms which bring about this influence, (2) establishing key relationships between these variables, and (3) providing the basis for developing an integrated theory to predict the hydrothermomechanical (HDTM) response of advanced composite structural components. The objective of this investigation is the development and description of an integrated theory for predicting the HDTM response of advanced composite structural components.

The approach pursued in developing this integrated theory consisted of the following: (1) review of work to date in order to select relationships between key hydrothermal variables (moisture and temperature) of resins and in order to identify and/or develop simple approximate relationships for relating resin physical and mechanical properties to the key hydrothermal variables, (2) performance of limited experiments to verify the conclusions arrived at from reviewing the work in (1), (3) incorporation of the simple relationships (identified in the literature or developed herein) as appropriate into composite micromechanics, composite macromechanics, laminate theory, and composite

structural analysis to complete the development of the desired integrated theory for the HDTM response, and (5) application of the integrated theory to selected examples and comparison with experimental data. Some of the governing equations are given in matrix notation in the text for convenience. Their expanded form is given in the Appendix.

EXPERIMENTAL INVESTIGATION

The experimental program was conducted to assess the effects of water absorption on the weights and volumes of an epoxy matrix resin and fiber/epoxy resin composites as well as to provide data to compare with composite micromechanic predictions.

Materials Investigated

The materials evaluated in this investigation consisted of neat PR-288 epoxy matrix resin and an AS-type graphite fiber/PR-288 resin unidirectional composite.

Materials Fabrication

The neat PR-288 epoxy matrix resin was supplied by the 3 M Company in plate form. The fiber/resin laminates were made at the Lewis Research Center using commercial AS-type graphite/PR-288 (AS/E) resin prepreg. Individual plies of prepreg were stacked in a metal mold to form 10 ply and 25 ply unidirectional laminates. A thermocouple was inserted into the laminate at one end. The cold mold was placed in a hydraulic laminating press previously heated to 450 K (350° F). The press platens were adjusted to apply contact pressure of 0.10 MPa (15 psi) on the mold. After the laminate temperature reached 311 K (100° F), contact pressure was maintained for another 3 minutes. The platen pressure was then increased gradually over a 2 minute period to 2.1 MPa (300 psi). The laminate was then cured at this pressure for a period of 2 hours. After completion of curing, the laminate was re-

moved from the press and the mold in a hot condition and allowed to cool at room temperature conditions.

Specimen Preparation and Testing

The neat epoxy resin and fiber/resin composite specimens were cut into test specimens using a diamond cutting wheel. The dimensions and designations of the specimens are given below.

Type and Dimensions	Designation
Neat Resin	
0.64 cm (0.25-in.) cube	Thick Resin
1.27 by 1.27 by 0.32 cm (0.50 by 0.50 by 0.125-in.)	Thin Resin
Fiber/Resin Composite	
10 ply - 1.27 by 1.27 by 0.13 cm (0.50 by 0.50 by 0.05-in.)	Thin Composite
25 ply - 1.27 by 1.27 by 0.25 cm (0.50 by 0.50 by 0.10-in.)	Thick Composite

Ten test specimens of each type were prepared and characterized for weight and physical dimensions in the as-cut condition.

All of the specimens were placed in a 339 K (150° F) oven to remove absorbed water and were allowed to remain in the oven until weights and dimensions were stabilized. The specimens were then subjected to room temperature [294 to 297 K (70° to 75° F) and approximately 50 percent relative humidity] and boiling water environments. The weights and dimensions of the specimens were periodically determined.

Results and Discussion

Figure 1 shows the effects of a boiling water moisture environment on the percentage changes in specimen volumes and weights for the thin epoxy resin specimens. These changes increased nonlinearly with time. Similar percentage changes for the thick epoxy resin specimens were

erratic and are not shown in figure 1. This erratic behavior is attributed to possible nonuniform moisture distribution through the specimen thickness.

Figure 2 shows the effects of a boiling water moisture environment on the percentage changes in specimen volumes and weights for the graphite fiber/epoxy resin composite specimens. The percentage changes for both the thick and thin composites increase nonlinearily with time. The percent changes in volume and weight for the thin specimen were essentially stabilized at the termination of the tests. However those of the thick composite were still changing gradually.

Figure 3 shows the relationships between the percentage changes in the volumes and weights of the specimens subjected to room temperature and boiling water environments, respectively. The slopes of the lines drawn through these data are equal to the coefficients listed in table I. The percentage dimensional changes versus weight changes (moisture expansion coefficients) are summarized in table II.

The points to be noted from figures 1 and 2 are that the absorbed moisture appears to have reached equilibrium in the thin resin and thin composite specimens, but not in the thick composite specimens. The moisture content in the resin at equilibrium is about 7.8 percent which is comparable to that reported in the literature (ref. 1). As can be seen both weight and volume changes are the same. The corresponding changes for the thin composite are about 3 percent. This is equivalent to about a 7 percent change in the amount of resin in the composite which is about 40 percent by volume.

The points to be noted from tables I and II are that the coefficients from the room temperature exposure specimens are 1 for the resin specimens and 0.3 for the composite specimens. The coefficients from the boiling water exposure are about 1.1 for all the specimens. This indicates that

the volume expansion of the resin in the composite is the same as in the next resin and also that the in situ moisture density is about the same as that of water.

THEORY, COMPARISONS, AND DISCUSSIONS

In this part of the paper are described the flow diagram of the integrated theory for hydrothermomechanical (HDTM) response, the concepts and assumptions for developing this theory, the key governing equations for composite micromechanics, composite macromechanics, and laminate theory. Finally, the incorporation of all of these into a computer code and the coupling of this code with a structural analysis procedure for predicting the HDTM response of advanced composite structural components are described. Comparisons are made with available data.

Flow Diagram of Integrated Theory for Hydrothermomechanical (HDTM) Response

The flow diagram of the integrated theory for HDTM response of composite components is illustrated schematically in figure 4. The key elements in this diagram are blocked with single lines while the desired result is blocked with double lines. As can be seen in the diagram the key elements are composite micromechanics, composite macromechanics, laminate analysis, and structural analysis. The desired result is the HDTM response of composite components. Each key element receives input from the element preceding it and supplies input to the element following it as well as additional information. In a design procedure the HDTM response must be compared to the appropriate design criteria in order to assess the adequacy of the composite component.

Concepts and Assumptions

The two concepts underlying this integrated theory are based on: (1) the observation that "the moisture affects the resin HDTM properties only," (refs. 1 to 5) and (2) the hypothesis that the moisture effects on

the resin HDTM properties can be expressed as a function of the use temperature and the reduced glass transition temperature of the wet resin (T_{gwr}). The reduced glass transition temperature (T_{gwr}) is related to both glass transition temperature of the dry resin (T_{gdr}) and the amount of moisture in the resin (m_r) as described in reference 6. This hypothesis implies isoparametric functional relationship between the various resin properties and may be expressed in symbolic form as follows:

$$\text{resin mechanical properties} \quad (E, G, S)_{wr} = F_1[(E, G, S)_{dr}, T_{gwr}] \tag{1}$$

$$\text{resin thermal properties} \quad (\alpha, K, C)_{wr} = F_2[(\alpha, K, C)_{dr}, T_{gwr}] \tag{2}$$

where E, ν, and S denote modulus, Poisson's ratio and fracture stress, respectively; and where α, K and C denote thermal expansion coefficient, heat conductivity and heat capacity, respectively. Moisture diffusivity and electrical conductivity are expected to have similar functional relationships. The glass transition temperature of the wet resin T_{gwr} is given in symbolic form as follows:

$$T_{gwr} = F_3 (T_{gdr}, m_r) \tag{3}$$

where, as mentioned previously, T_{gdr}, and m_r denote glass transition temperature of the dry resin and m_r the moisture content in the resin. (See ref. 6 for the functional form of F_3).

The following assumptions were made in developing this integrated theory: (1) the moisture diffusion in the composite is independent of the stress state, (2) the temperature distribution in the composite is independent of the stress state. (3) all the assumptions that are common to composite

linear micromechanics and macromechanics, and linear laminate theory; (4) the moisture effects in the composite are manifested through the resin as described by micromechanics; and (5) the hydrothermomechanical response of the composite structural component may be determined by solving the appropriate moisture diffusion, heat transfer, and structural problems as will be indicated later.

Relationships for Wet Resin Properties

The relationships among the wet resin mechanical properties and the room temperature dry properties and temperature (eq. (1)) were determined in this investigation using the following procedure: (1) retention ratios (wet property at test temperature divided by room temperature dry property) of wet resin and unidirectional composite properties from the literature (refs. 1, 4, 7, and 8) were plotted versus temperature, (2) a simple algebraic expression was sought to approximate the retention ratio and thereby establish the functional relationship F_1 in equation (1). The motivation for seeking a simple algebraic expression is that this can readily be incorporated into available composite micromechanics equations. The procedure used to establish the relationship is illustrated in figure 5. As can be seen the simple algebraic relationship

$$\frac{\text{wet resin mechanical property at test temperature}}{\text{dry resin mechanical property at room temperature}} = \mathcal{F}_m \approx \left[\frac{T_s - T}{T_s - T_o}\right]^{1/2} \tag{4}$$

is a good approximation of the data in the range 200 K (-100° F) $< T < T_s$. The notation in equation (4) is as follows: $\mathcal{F}_m$ denotes mechanical property retention ratio, T_s equals T_{gwr}, T is the use temperature and T_o equals 273 K (0° C). The temperatures are expressed in K. The moisture effect is incorporated through T_s as defined in equation (3). The

corresponding relationship for the wet resin thermal properties is assumed to be the inverse of the equation (4) or

$$\frac{\text{wet resin thermal property at test temperature}}{\text{dry resin thermal property at room temperature}} = \mathcal{f}_t \approx \left[\frac{T_s - T_o}{T_s - T}\right]^{1/2} \tag{5}$$

Equation (5) is a good approximation for the literature dry resin data (refs. 9 and 10) in the range 200 K (-100^{o} F) $< T < T_s$ as is shown in figure 6. It is anticipated that equation (5) will fit wet resin thermal properties equally as well in the same range. If it does not, another relationship may be found and the procedure described below can be used to incorporate the moisture effects thermal properties. Summarizing then:

$$(E, G, S)_{wr} = (E, G, S)_{ro}\ \mathcal{f}_m \tag{6}$$

$$(\alpha, K, C)_{wr} = (\alpha, K, C)_{ro}\ \mathcal{f}_t \tag{7}$$

where the subscript ro refers to dry resin properties evaluated at room temperature; and $\mathcal{f}_m$ and $\mathcal{f}_t$ are given by equations (4) and (5), respectively.

Composite Micromechanics

The governing micromechanics equations which incorporate the moisture effects in the unidirectional composite (ply) response were derived using the procedures of references 11, 12, and 13. Since the number of these equations can be very large (refs. 14 and 15) herein we present those equations which are either used to predict results or are used to illustrate important phenomena.

Volume and density relationships. - The ply density ($\rho_{\ell w}$) and ply moisture (m_ℓ) are given by:

$$\rho_{\ell w} = \rho_{\ell d} + (\rho_{\ell d} + k_v \rho_m)(3\,\beta_r k_r + k_v)\, m_r \tag{8}$$

$$m_{\ell} = (3\beta_r k_r + k_v)\, m_r \rho_{nl} / \rho_{fd} \tag{9}$$

where:

$$\rho_{fd} = k_f \rho_f + k_r \rho_r \tag{10}$$

$$\beta_r = \frac{1}{3}\left[(\rho_{rd}/\rho_m) - k_v\right. \tag{11}$$

$$1 = k_f + k_r + k_v \tag{12}$$

and where the notation in equations (8) to (12) is as follows: ρ denotes density; k, actual volume ratio; m, moisture; β, moisture expansion coefficient; the subscripts f, r, v, and ℓ denote fiber, resin, void, and ply property, respectively; and the subscripts d and w denote dry and wet conditions, respectively. The presence of voids affects all the properties given by equations (8) to (11). Note that equation (11) can be used to predict the theoretical moisture expansion coefficient of the resin by setting $k_v = 0$. For example, typical resins have specific gravities of about 1.2. The theoretical volumetric expansion coefficient of those resins is $3\beta_r$ which is equal to the specific gravity of the resins or 1.2 in this example and is in good agreement with the measured coefficient of 1.1 of the boiling exposure specimens in table I. The value of β_r of about 0.4 is also in good agreement with literature data (ref. 1). Equation (9) predicts a moisture content of about 2.6 percent for an AS/PR-288 composite compared to about 2.9- percent for the thin composite and 2.3-percent for the thick composite from figure 2. These comparisons show that the values predicted by equations (9) to (11) are in good agreement with measured data. They also show that the resin volume expansion is conserved in the composite as the composite expands at these moisture contents. This means that the resin is essentially incompressible and will probably behave like a viscoelastic or

viscoplastic medium. A direct conclusion from this condition is that microstress relaxation occurs in the composite. Another conclusion is that the voids in the in situ resin may collapse at the high (about 1-percent and greater) moisture content.

Ply elastic constants. - The governing micromechanics equations for predicting the ply elastic properties longitudinal modulus ($E_{\ell 11}$), transverse modulus ($E_{\ell 22}$), major Poisson's ratios ($\nu_{\ell 12}$) and intralaminar shear modulus ($G_{\ell 12}$), respectively, are:

$$E_{\ell 11} = k_f E_{f11} + k_r \mathscr{E}_m E_{ro} \tag{13}$$

$$E_{\ell 22} = \frac{\mathscr{E}_m E_{ro}}{1 - \sqrt{k_f}\,(1 - \mathscr{E}_m E_{ro}/E_{f22})} \tag{14}$$

$$\nu_{\ell 12} = k_f \nu_{f12} + k_r \nu_{ro} \tag{15}$$

$$G_{\ell 12} = \frac{\mathscr{E}_m G_{ro}}{1 - \sqrt{k_f}\,(1 - \mathscr{E}_m G_{ro}/G_{f12})} \tag{16}$$

where

$$G_{ro} = \frac{E_{ro}}{2(1 + \nu_{ro})} \tag{17}$$

and where $\mathscr{E}_m$ is given by equation (4); the subscript f denotes fiber property; the subscripts 1 and 2 denote fiber directions with 1 taken along the fiber and 2 transverse to the fiber direction. Note that the major Poisson's ratio is independent of moisture as may be verified from equation (17).

Ply expansivities. - The thermal expansion coefficients ($\alpha_{\ell 11}$

and $\alpha_{\ell 22}$) and the moisture expansion coefficients or swelling coefficients ($\beta_{\ell 11}$ and $\beta_{\ell 22}$) are given, respectively, by the following micromechanics equations:

$$\alpha_{\ell 11} = \frac{\alpha_{ro} \mathcal{F}_t E_{ro} \mathcal{F}_m k_r + \alpha_{f11} k_f E_{f11}}{\mathcal{F}_m E_{ro} k_r + E_{f11} k_{f11}} \tag{18}$$

$$\alpha_{\ell 22} = \alpha_{ro} \mathcal{F}_t (1 - \sqrt{k_f})(1 + k_f \nu_{ro} E_{f11}/E_{\ell 11}) + \alpha_{f22} \sqrt{k_f} \tag{19}$$

$$\beta_{\ell 11} = \beta_r k_r \mathcal{F}_m E_{ro}/E_{\ell 11} \tag{20}$$

$$\beta_{\ell 22} = (1 - \sqrt{k_f})\, \beta_r \left[1 + \frac{\sqrt{k_f}\,(1 - \sqrt{k_f})\, \mathcal{F}_m E_{ro}}{\sqrt{k_f} E_{\ell 22} + (1 - \sqrt{k_f}) \mathcal{F}_m E_{ro}}\right] \tag{21}$$

or for incompressible resin with $\beta_{\ell 11} \approx 0$.

$$\beta_{\ell 22} = \beta_{\ell 33} = \frac{3 \beta_r k_r \rho_{\ell d}}{(3 \beta_r k_r + k_v) \rho_m} \tag{22}$$

where $\mathcal{F}_m$ is given in equation (4) and $\mathcal{F}_t$ in equation (5). At small moisture (less than 0.3 percent) contents $\beta_{\ell 22}$ is probably closer to the value predicted by equation (21) than equation (22) which was derived assuming conservation of volume of the in situ resin.

Ply uniaxial strengths. - The uniaxial ply strengths, tranverse tension ($S_{\ell 22T}$) and compression ($S_{\ell 22C}$) and intralaminar (in-plane) shear ($S_{\ell 12S}$) are given, respectively, by the following micromechanics equations:

$$S_{\ell 22T} = \beta_{22T}\left(\frac{S_{rTo}}{E_{ro}}\right)\left(\frac{E_{\ell 22}}{\beta_v \varphi_{\mu 22}}\right) \tag{23}$$

$$S_{\ell 22C} = \beta_{22C}\left(\frac{S_{rCo}}{S_{rTo}}\right)\left(\frac{E_{\ell 22}}{\beta_v \varphi_{\mu 22}}\right) \tag{24}$$

$$S_{\ell 12S} = \beta_{12S}\left(\frac{S_{rSo}}{G_{ro}}\right)\left(\frac{G_{\ell 12}}{\beta_v \varphi_{\mu 12}}\right) \tag{25}$$

where β_v denotes void magnification factor and φ_μ strain magnification factor, S denotes fracture stress; the subscripts T, C, and S denote tension, compression and shear, respectively. The coefficient β_{22T}, β_{22C}, and β_{12S} are correlation coefficients if needed, otherwise they are assumed to be unity. The void and strain magnification factors are given by:

$$\beta_v = 1/\left[1 - (4k_v/\pi k_r)\right]^{1/2} \tag{26}$$

$$\varphi_{\mu 22} = \frac{1 - \sqrt{k_f}\, E_{\ell 22}/E_{f22}}{1 - \sqrt{k_f}} \tag{27}$$

$$\varphi_{\mu 12} = \frac{1 - \sqrt{k_f}\, G_{\ell 12}/G_{f12}}{1 - \sqrt{k_f}} \tag{28}$$

The uniaxial ply longitudinal tensile strength ($S_{\ell 11T}$) and compressive ($S_{\ell 11C}$) are given by:

$$S_{\ell 11T} = S_{fT}\,\beta_{fT} k_f + k_r \mathcal{F}_m E_{ro}/E_{f11} \tag{29}$$

$$S_{\ell 11C} = \frac{1}{2}\left[S_{fC}\left(\beta_{fc} k_f + k_r \mathcal{F}_m E_{ro}/E_{f11}\right) + \left(\beta_{CS} S_{\ell 12S} + S_{rCo}\right)\right] \qquad (30)$$

where S_{fT} and S_{fC} denote fiber longitudinal tensile and compressive strength, respectively; the coefficients β_{fT} and β_{fC} are correlation coefficients if needed, otherwise taken equal to unity; $\mathcal{F}_m$ is given by equation (4) and $S_{\ell 12S}$ by equation (25). It is important that the various correlation coefficients in equations (23), (24), (25), (29), and (3) be evaluated from dry room temperature data and should remain invariant with both temperature and moisture changes. These coefficients as well as β_{CS} in equation (30), are evaluated using the procedure described in reference 12. Though a specific set of micromechanics equations were used herein, the functional relations $\mathcal{F}_m$ and $\mathcal{F}_t$ should work equally well with any other set.

Comparisons with measured data. - The unidirectional (ply) properties predicted by micromechanics for an AS/3501-5 composite, using the fiber and resin properties given in table III are tabulated together with literature data (ref. 8) in table IV. The properties are for one moisture content (1.8 percent) and two temperatures (room and 366 K (200° F)). By comparing corresponding measured and predicted properties it is seen that the agreement is about 10-percent, which is considered very good, for most of the properties except $S_{\ell 11C}$ at room temperature, $S_{\ell 12S}$ at both temperatures, and $E_{\ell 22}$ and $G_{\ell 12}$ at 366 K (200° F)). One explanation may be the normal difficulties encountered in measuring these properties. There is no measured wet data for the thermal expansion coefficients.

The predicted value for $\beta_{\ell 11}$ from equation (20) with $\beta_r \approx 0.41$, $k_r = 0.4$ and $\mathcal{F}_m E_{ro}/E_{\ell 11} \approx 0.0205$ is about 0.04 compared with 0.05 for the thin composite and with 0.02 for the thick composite, table II. This difference may be due to possible irreversible damage induced in the resin during cooling down. The predicted value for $\beta_{\ell 22}$ using equation (22) with $k_v = 0$, and $\rho_{\ell d}/\rho_m = 1.58$ is about 0.79. This is in good agreement (within 2-percent) with the averages of the thickness and width moisture expansion coefficients for the thin specimen, 0.75, and for the thick specimen, 0.80 (table II).

The significant result from these comparisons is that the micromechanics equations predict ply HDTM properties which are in good agreement with measured data at different hydrothermal environments. This agreement leads to the conclusion that the micromechanics equations given herein may be used to assess the composite response in different hydrothermal environments for preliminary design. Another significant conclusion is that the moisture resistance of various resins including new ones may be assessed by measuring the room temperature properties given in table III and those properties required to determine T_s.

Composite Macromechanics

The governing macromechanics equations pertinent to this discussion are the ply HDTM relationships and the ply combined-stress failure criteria. The ply HDTM relationships in matrix form are given by

$$\{\epsilon_\ell\} = [E_\ell]^{-1} \{\sigma_\ell\} + \Delta T_\ell \{\alpha_\ell\} + m_\ell \{\beta_\ell\} \tag{31}$$

where $\{\ \}$ denotes a 3×1 vector and $[\ ]$ a 3×3 array, their expanded form is indicated in the appendix. ΔT_ℓ and m_ℓ denote the ply tem-

perature and moisture respectively. Equation (31) may be solved for σ_ℓ if needed. Equation (31) is written about the ply material axes (1,2,3) with 1 along the fiber 2 transverse to it, and 3 through the thickness. Equation (31) may be transformed to any other axes by well known transformations (refs. 10, 14, 16). Note the similarity between $\Delta T_\ell \{\alpha_\ell\}$ and $m_\ell \{\beta_\ell\}$. This similarity offers the following two features: (1) these terms are computationally interchangeable, and (2) they may be combined on an element by element basis. These two features make it possible to use available computer codes which include only the ΔT_ℓ term to predict the HDTM response of angleplied laminates. Reference 14 provides such a computer code and an integrated theory for the structural response of angleplied laminates subjected to thermal and mechanical loads. This code can also be applied to the integrated theory for the HDTM response of angleplied laminates by incorporating: (1) the two above features and (2) the moisture effects through the micromechanics equations described previously.

The ply combined-stress failure criterion used in this investigation is that developed in-house (LeRC combined stress failure criterion which is described in ref. 12) and is available in the computer code (ref. 14).

Laminate Analysis

Governing equations. - The laminate analysis part of the integrated theory for predicting the HDTM response of composite components is available in the computer code (ref. 14). The governing laminate analysis equations include those for predicting the HDTM response of the laminate and those for predicting the ply HDTM strains and stresses. The equations for the laminate HDTM response are:

$$\left\{\begin{array}{c} N_c \\ \hline M_c \end{array}\right\} = \left[\begin{array}{c|c} A_c & C_c \\ \hline C_c & D_c \end{array}\right] \left\{\begin{array}{c} \epsilon_{co} \\ \hline -\kappa_c \end{array}\right\} - \left\{\begin{array}{c} N_{ct} \\ \hline M_{ct} \end{array}\right\} - \left\{\begin{array}{c} N_{cm} \\ \hline M_{cm} \end{array}\right\} \tag{32}$$

where N, M, ϵ, κ are 3×1 vectors (see appendix for expanded form) denoting, respectively: inplane force, bending moment, reference plane strains, and local curvatures; A_c, C_c, and D_c, are 3×3 arrays denoting; axial, coupled, and bending stiffness, respectively. These arrays are determined from ply properties using laminate analysis procedures (refs. 8, 14, and 16). The subscript c denotes composite (laminate) property or variable, and the subscripts m and t denote moisture and thermal properties. Note that N_{ct} and M_{ct} are the thermal forces and moments and N_{cm} and M_{cm} are the hydro forces and moments. Equation (32) is an important result of laminate theory and is generally used to predict the following:

1. HDTM laminate relationships required in structural analysis.
2. Laminate forces (displacements) when the displacements (forces) are known from structural analysis
3. Ply HDTM stresses
4. Residual and hydro stresses
5. Laminate warpage from hydrothermal stresses.

The ply HDTM strain and stresses are, respectively, given by:

$$\{\epsilon_\ell\} = [R_{\ell\epsilon}] \langle \{\epsilon_{co}\} - z_\ell \{\epsilon_{cO}\} - z_\ell \{\kappa_c\} \rangle \tag{33}$$

$$\{\sigma_\ell\} = [E_\ell] \langle [R_{\ell\epsilon}] \{\epsilon_\ell\} - m_\ell \{\beta_\ell\} - \Delta T_\ell \{\alpha_\ell\} \rangle \tag{34}$$

where $R_{\ell\epsilon}$ is a 3×3 strain transformation matrix which is a function

of θ measured from the laminate structural axes to the ply material axis (see appendix for expanded form), and z_ℓ is the normal distance from the reference plane to the center of the ply. The ply hydrothermal strains and stresses for symmetric laminates with uniform temperature and moisture conditions are, respectively, given by:

$$\{\epsilon_{\ell HT}\} = m\langle[R_{\ell\epsilon}]\{\beta_c\} - \{\beta_\ell\}\rangle + \Delta T\langle[R_{\ell\epsilon}]\{\alpha_c\} - \{\alpha_\ell\}\rangle \quad (35)$$

$$\{\sigma_{\ell HT}\} = [E_\ell]\langle m\langle[R_{\ell\epsilon}]\{\beta_c\} - \{\beta_\ell\}\rangle + \Delta T\langle[R_{\ell\epsilon}]\{\alpha_c\} - \{\alpha_\ell\}\rangle\rangle \quad (36)$$

where the subscript HT denotes hydrothermal property and the other symbols have been previously defined. As can be observed from equations (35) and (36) combination of moisture (m) and temperature (ΔT) may exist which will result in zero hydrothermal strains and stresses. As can also be observed hydrothermal environments when both moisture and temperature increase or decrease induce the largest hydrothermal strains or stresses.

Application - laminate elastic properties. - The laminate analysis just described was used to analyze some of the laminates tested in reference 8. The results obtained for elastic properties are summarized in table V. The comparisons show that the predicted values are in good agreement with measured data (within 10 percent) except for the shear moduli of laminates I and II where the predicted values are 18 and 15 percent higher, respectively. A possible reason for this large difference is inaccuracy of the experimental values arising from the difficulty in measuring shear properties.

Application - hydrothermomechanical stresses. - The predicted ply

HDTM stresses for one of these laminates are summarized in bar-chart form in figure 7, both individually and combined. The uniaxial strengths are also shown. The following points are worthy of note in figure 7:

1. The hydro and residual stresses have opposite signs with the hydro stress dominating (about 3-times as high for some stresses).

2. The hydro and mechanical stresses have the same sign for the longitudinal and transverse stresses in the 45° plies and the transverse stress in the 0° plies.

3. The mechanical load is the dominant source of the shear stress in the 45° plies.

4. The transverse residual stress magnitude is about equal to the uniaxial transverse strength in the 0° and 45° plies. It is possible that this stress caused transply cracking in these plies prior to moisture conditioning of the laminate.

5. The mechanical load shear stress in the 45° plies exceeds the corresponding uniaxial strength ($S_{(12S)}$).

6. The hydrothermal stress contribution to the longitudinal stress in the 0° plies is negligible compared to mechanical stress.

7. It appears that fracture was initiated by shear failures of the 45° plies and completed when the 0° plies failed in longitudinal tension.

One important conclusion from the above discussion is that the ply hydrothermal stresses in angleplied laminates are substantial and need to be considered in both analysis and design.

Application - laminate fracture. - Predicted laminate fracture stresses for combined HDTM load conditions are compared with measured data (ref. 8) using a bar-chart in figure 8. Note in this

figure both measured data ranges and predicted ranges are shown by horizontal lines in the bars. The lower bound of the predicted fracture stress is based on first ply failure (usually induced by transverse or shear stress) while the upper bound is based on failure of the remaining major load carrying plies (not necessarily fiber fractures). The predicted fracture stresses are based on room-temperature-dry uniaxial ply strengths and room-temperature-wet ply hydrothermal elastic properties. This was done for two reasons: (1) the lower bound on laminate fracture stress predicted using room-temperature-wet ply strengths was considered to be unrealistically low and, (2) to compensate for possible in situ ply transverse and intralaminar shear strengths which are suspected to be higher than the uniaxial values tested under the same HDTM environment.

Examining the bars in figure 8, it is seen that the measured and predicted ranges overlap in 13 of the 15 cases. The two cases where they do not overlap are laminate 1 under longitudinal tension and under longitudinal compression. In both of these cases the predicted values are lower than the measured data by about the same amount. One reason the predicted longitudinal compression fracture stress is lower may be the in situ enhancement of the ply longitudinal compressive strength.

The important observation from the data in figure 8 is that dry ply strength data should be used to predict laminate fracture stresses in order to obtain reasonable agreement with the measured data. Another one is that the predicted lower bound on fracture stress appears to be on the conservative side. The results of this stress analysis show that the LeRC ply combined-stress strength criterion can be used for pre-

dicting laminate fracture under combined HDTM loads. One significant conclusion from the previous discussion is that the in situ ply strengths may be higher than those determined under uniaxial tests.

Application - hydrostresses. - Theoretical ply transverse hydrostresses in $(\theta/0/-\theta/0)_s$ laminates of different composite systems are shown in figure 9 as a function of θ. These hydrostresses correspond to 2.5 percent moisture and were predicted using equation (36) with $\Delta T = 0$ and $m = 0.025$. As can be seen from the curves in figure 9 the transverse hydrostresses are compressive, increase with increasing θ and leveling at about $\theta = 60^{\circ}$, and are sensitive to composite system, ranging from about 0.034 GPa (5 ksi) for Kevlar/epoxy (KEV/E) to about 0.19 GPa (28 ksi) for boron/epoxy (B/E). The corresponding intralaminar shear stresses are shown in figure 10. The intralaminar shear stress increases very rapidly with θ peaking at about $\theta = 45^{\circ}$. It is sensitive to composite system ranging from about 0.014 GPa (2 ksi) for KEV/E to 0.083 GPa (12 ksi) for B/E.

Comparable plots in $|\pm\theta|_s$ laminates are shown in figure 11 for transverse stress and in figure 12 for intralaminar shear. In these laminates the ply transverse hydrostress increases very rapidly, with θ peaking at 45°, and is symmetric about 45°. It is strongly influenced by the composite system ranging from about 0.034 GPa (5 ksi) for KEV/E to about 0.19 GPa (28 ksi) for B/E. Note that these ranges are about the same as those for the $|\theta/0/-\theta/0|_s$ except that the variation with θ is different. The corresponding intralaminar shear stresses are shown in figure 12. This stress is antisymmetric with respect to 45°, has two peaks at about $\theta = 30^{\circ}$ and $\theta = 60^{\circ}$, and depends on the composite system, ranging from about 0.014 GPa (2 ksi) for KEV/E to about 0.069 GPa (10 ksi) for B/E or S-glass/epoxy (S-G/E).

The major conclusion to be drawn from the above hydrostress results is that the transverse stresses are compressive in an increasingly uniform moisture environment and as such they may enhance the ply in situ transverse strength.

The ply hydro stresses induced in a B/E unidirectional laminate during moisture absorption are shown in figure 13 and during desorption in figure 14. The moisture profiles used in these predictions were obtained from reference 1. The curves show that large transverse stresses can be induced. These stresses are compressive in the outer plies and tensile in the inner plies during moisture absorption. During desorption the transverse stress is tensile in the outer and center plies and compressive in the intermediate plies. The longitudinal stress is negligible for both cases. Note that curves for both stresses have the same but reflected shape of the moisture curve. The magnitude of the transverse tensile stress is about 0.090 GPa (13 ksi) for the absorption case and is about 0.048 GPa (7 ksi) for the desorption case compared to the corresponding strength of about 0.055 GPa (8 ksi). One conclusion from these results is that rapid moisture absorption or desorption may induce transply cracks. For a more extensive discussion on hydro stresses see reference 17.

Structural Analysis

The structural analysis part of the integrated theory described herein consists of the coupling of the composite mechanics computer code (ref. 14) with a general purpose finite element structural analysis program, for example, NASTRAN (ref. 18). Referring to figure 4 the integrated theory for the HDTM response is completed when the laminate analysis supplies the material properties (eq. (32)) required

in NASTRAN to generate the element stiffness, and when NASTRAN predictes the HDTM structural response displacement vector (ϵ_{c0} and κ_c, eq. (32)) required by laminate theory to perform the laminate stress analysis.

A simple example of HDTM structure response of a composite component is the free warpage of an angleplied laminate subjected to nonuniform moisture distribution through the thickness. One way to assess this warpage is to fix the laminate at one corner and determine the lateral displacement at the diagonally-opposite corner. This structural response may also be predicted by the following close form equation for a rectangular flat laminate

$$w = \frac{1}{2}\left(a^2\kappa_{cxx} + b^2\kappa_{cyy} + 2\,ab\kappa_{cxy}\right) \tag{37}$$

where w is the corner displacement, a and b the side dimension, and κ_c are the local curvatures which are determined from equation (32). Corner displacements obtained for a square laminate a = b = 25.4 cm (a = b = 10 in.) for two laminate configurations $[(\pm 30)_2]_s$ and $[30/0/-30/0]_s$ from an AS/E composite and subjected to three different nonuniform through-the-thickness moisture profiles are summarized in figure 15. As can be seen in this figure the corner displacement due to warpage induced by moisture can be substantial. Note that corner displacements greater than 2.54 cm (1-in.) are probably beyond the limits of linear structural analysis. It is interesting to note that the linear and parabolic moisture profiles induce approximately the same warpage.

The variation of the warpage corner displacement as a function of ply angle is shown in figure 16 for laminates with hyperbolic moisture profiles. Note that the warpage is sensitive to laminate configuration and is sensitive to certain moisture profiles. One conclusion from this dis-

cussion is to take advantage of these sensitivities to assess stress relaxation due to viscoelastic (viscoplastic) behavior of moist resins.

CONCLUSIONS

The major results and conclusions of an investigation to provide an integrated theory for predicting the hydrothermomechanical (HDTM) response of advanced composite components are as follows:

1. An integrated theory was developed to predict the HDTM response of advanced composite components. This theory incorporates the hydrothermal effects in composites through micromechanics, macromechanics and laminate analysis all of which are parts of a composite mechanics computer code. The computer code is coupled with a major structural analysis finite element computer program to complete the integrated theory.

2. A simple relationship was established which relates the mechanical properties of the wet resin to its room temperature dry properties and to its wet glass-transition temperature. The corresponding thermal properties relationship is the reciprocal of the mechanical properties relationship.

3. The resin conserves its volume in a hydro environment. The density of the in situ moisture is about the same as water. Voids in the in situ resin may collapse at high moisture contents (greater than 1-percent).

4. Composite micromechanics predicts hydro expansion and ply mechanical properties (elastic and strength) which are generally in good agreement with measured data under different hydrothermal environments.

5. Laminate theory predicts laminate wet properties which are within 10-percent of measured data.

6. Laminate theory in conjunction with the LeRC failure criterion

predicts laminate fracture stress ranges which overlap with those of the measured data. The predicted lower bound on fracture stress tends to be below the measured data scatter in general.

7. The hydro stresses in the plies of angleplied laminates reach magnitudes in the transverse direction and in intralaminar shear which are comparable to corresponding ply strengths.

8. The ply hydro transverse stress is either tensile or compression depending on whether moisture is absorbed or desorbed. The profiles of ply stresses through-the-thickness of the laminate are mirror images of the corresponding moisture profile. The ply hydro stresses depend on moisture content and profile, laminate configuration and composite system. KEV/E angleplied laminates have the lowest ply hydro stress and B/E or S-G/E the highest.

9. Nonuninform moisture through the laminate thickness induces severe laminate warpage. This warpage depends on laminate configuration and can produce corner displacements several times the laminate thickness.

10. Hydro stress in angleplied laminates can be predicted using the equivalance feature between hydro and thermal expansions.

11. In situ ply strength may be enhanced by hydrothermal environments as compared with uniaxial data. The in situ resin may behave like a viscoelastic or viscoplastic medium in hydrothermal environments. Moisture induced warpage in angleplied laminates may be an effective means to assess stress relaxation in a hydrothermal environment.

APPENDIX

(Vector and array expansion)

$$\{\epsilon_\ell\}^T = [\epsilon_\ell] = [\epsilon_{\ell 11},\ \epsilon_{\ell 22},\ \epsilon_{\ell 12}]$$

and similarly for all other vectors.

$$[E_\ell]^{-1} = \begin{bmatrix} 1/E_{\ell 11} & -\nu_{\ell 21}/E_{\ell 22} & 0 \\ -\nu_{\ell 12}/E_{\ell 22} & 1/E_{\ell 22} & 0 \\ 0 & 0 & 1/G_{\ell 12} \end{bmatrix}$$

$$[A_C] = \begin{matrix} A_{c11} & A_{c12} & A_{c13} \\ A_{c21} & A_{c22} & A_{c23} \\ A_{c31} & A_{c32} & A_{c33} \end{matrix}$$

and similarly for $[E_c]$, $[C_c]$, and $[D_c]$.

$$\{N_c\}^T = [N_c] = [N_{cxx},\ N_{cyy},\ N_{cxy}]$$

and similarly for $\{N_{ct}\}$, $\{N_{cm}\}$, $\{M_c\}$, $\{M_{ct}\}$, and $\{M_{cm}\}$.

$$[R_{\ell\sigma}]^{-1} = [R_{\ell\epsilon}]^T = \begin{matrix} \cos^2\theta & \sin^2\theta & -\sin 2\theta \\ \sin^2\theta & \cos^2\theta & \sin 2\theta \\ \frac{1}{2}\sin 2\theta & -\frac{1}{2}\sin 2\theta & \cos 2\theta \end{matrix}$$

REFERENCES

1. Anon, "Air Force Workshop on Durability Characteristics of Resin Matrix Composites at Battelle's Columbus Laboratories," Sept. 30 and Oct. 1-2, 1975.

2. Vinson, Jr. R. et al., "The Effects of Relative Humidity and Elevated Temperature on Composite Structures. (AFOSR-TR-77-0030), Bolling A. F. B., Washington, D.C., Dec. 1976.

3. Anon, Mechanics of Composites Review, January 28-29, 1976. Air Force Materials Laboratory, Nonmetallic Materials Division Bergamo Center, Dayton, Ohio, 1976.

4. Anon, Mechanics of Composites Review, October 26-28, 1976. Air Force Materials Laboratory, Nonmetallic Materials Division and Air Force Office of Scientific Research Directorate of Aerospace Sciences. Stratford House, Dayton, Ohio, 1976.

5. Christian, J. L., et al., "Environmental Effects on Advanced Composite Materials (ASTM-STP 602) American Society For Testing and Materials, Philadelphia, Pa., 1976.

6. Browning, C.E., "The Mechanics of Elevated Temperature Property Losses in High Performance Structural Epoxy Resin Matrix Materials After Exposure to High Humidity Environments," (AFML-TR-76-153) Wright-Patterson Air Force Base, Ohio, March 1977.

7. Altman, J. M., et al., "Composite, Low-Cost Secondary Airframe Structures," (AFFDL-TR-76-4, Vol. 1) Wright-Patterson Air Force Base, Ohio, August 1976.

8. Verette, R. M. and Labor, J. D., "Structural Criteria for Advanced Composites," (AFFDL-TR-76-142, Vol. 1), Wright-Patterson Air Force Base, Ohio, March 1977.

9. Daniel, I. M. and Liber, T., "Lamination Residual Stresses in Hybrid Composites," Final Report - Part 1. (NASA CR-135085, IITRID 06073-11), 1976.

10. Anon, Advanced Composites Design Guide, Vol. 2, Analysis, Wright-Patterson Air Force Base, Ohio, 1973.

11. Chamis, C. C., "Thermoelastic Properties of Unidirectional Filamentary Composites by a Semiempirical Micromechanics Theory," (Science of Advanced Materials and Process Engineering Proceedings, Vol. 14), Western Periodicals Co., 1968.

12. Chamis, C. C. "Failure Criteria for Filamentary Composites," (ASTM-STP 460) American Society for Testing and Materials, Philadelphia, Pa., 1970.

13. Chamis, C. C., "Micromechanics Strength Theories," in Broutman, Broutman, L. J., "Composite Materials," Vol. 5, "Fracture and Fatigue." Academic Press, New York, 1974, pp. 93-151.

14. Chamis, C. C., "Computer Code for The Analysis of Multilayered Fiber Composites - Users Manual," NASA TN D-7013, National Aeronautics and Space Administration, 1971.

15. Chamis, C. C., "Computerized Multilevel Analysis for Multilayered Fiber Composites," (Computers and Structures, Vol. 3, Pergamon Press), Great Britain, 1973, pp. 467-482.

16. Ashton, J. E , Halpin, J. C., and Petit, P. H., "Primer on Composite Materials: Analysis," Progress in Materials Science Series, Vol. 3, Technomic Publishing Co., Stanford Conn., 1969.

17. Pipes, B. R., Vinson, J. R., and Chou, T. W., "On the Hygrothermal Response of Laminated Composite Systems." Journal of Composite Materials, Vol. 18, 1975, p. 126.

18. McCormic, C. W., "NASTRAN User's Manual (Level 15)," NASA Special Publication 222 (01), 1972.

TABLE I. - MOISTURE EXPANSION VOLUME COEFFICIENTS FOR EPOXY RESIN AND FIBER/RESIN COMPOSITE SPECIMENS

Specimen	Coefficient
Room temperature	
Thin resin	1.0
Thick resin	1.0
Thin composite	.3
Thick composite	.3
Boiling water	
Thin resin	1.0
Thick resin	1.1
Thin composite	1.2
Thick composite	1.1

E-3272

TABLE II. - MOISTURE EXPANSION COEFFICIENTS FOR LINEAL DIMENSIONS FOR FIBER/RESIN COMPOSITE SPECIMENS

Specimen	Coefficients			
	Specimen directions			
	Length	Width	Thickness	Average thickness width
Thin composite	0.05	0.5	1.0	0.79
Thick composite	0.02	0.9	0.7	0.80

TABLE III. - FIBER AND RESIN PROPERTIES AND COEFFICIENTS USED IN THE MICROMECHANICS EQUATIONS

Property	Symbol	Units SI (English)	Value
AS graphite fiber			
Longitudinal modulus	E_{F11}	GPa (MSI)	221 (32)
Transverse modulus	E_{F22}	GPa (MSI)	13.8 (2.0)
Shear modulus	G_{F12}	GPa (MSI)	13.8 (2.0)
Poisson's ratio	ν_{F12}	---	0.2
Longitudinal thermal exp. coeff.	α_{F11}	$^{o}K^{-1}(^{o}F^{-1})$	-1×10^{-6} (-0.56×10^{-6})
Transverse thermal exp. coeff.	α_{F22}	$^{o}K^{-1}(^{o}F^{-1})$	1×10^{-5} (5.6×10^{-6})
Longitudinal tensile strength	S_{FT}	GPa (KSI)	2.7 (400)
Longitudinal compression	S_{FC}	GPa (KSI)	2.7 (400)
3501-5 Resin room temperature (ref. 8) dry			
Modulus	E_{ro}	GPa (MSI)	4.1 (0.4)
Poisson's ratio	ν_{ro}	---	0.4
Thermal exp. coeff.	α_{ro}	$^{o}K^{-1}(^{o}F^{-1})$	5.7×10^{-5} (32×10^{-6})
Moisture exp. coeff.	β_{r}	---	0.4
Tensile strength	S_{rTo}	GPa (KSI)	0.048 (7.0)
Compression strength	S_{rCo}	GPa (KSI)	0.25 (36.3)
Shear strength	S_{rso}	GPa (KSI)	0.048 (7.0)
Coefficients			
β_{CS} equation (30)	----	---	12.1

TABLE IV. - COMPARISON OF MEASURED AND PREDICTED MECHANICAL PROPERTIES OF ANGLEPLIED LAMINATES AS/3501-5 IN HYDROTHERMAL ENVIRONMENTS

Property	Symbol	Units SI (English)	Properties with 1.8 percent moisture			
			Room temperature		200° F	
			Measured*	Predicted	Measured*	Predicted
Density	ρ_f	kgm/m^3 (lb/in.^{3})	----------	1.6×10^4 (0.57)	----------	1.6×10^4 (0.57)
Longitudinal modulus	E_{f11}	GPa (MSI)	131 (19.1)	133 (19.4)	135 (19.5)	133 (19.3)
Transverse modulus	E_{f22}	GPa (MSI)	8.6 (1.25)	7.25 (1.05)	4.21 (0.61)	5.18 (0.75)
Shear modulus	G_{f12}	GPa (MSI)	3.73 (0.54)	3.52 (0.51)	1.73 (0.25)	2.28 (0.33)
Poisson's ratio	ν_f	----------	0.30	0.28	----------	0.28
Temp. expansion coeff.	α_{f11}	K^{-1} ($^oF^{-1}$)	----------	-5.6×10^{-7} (-0.31×10^{-6})	----------	-4.0×10^{-7} (-0.22×10^{-6})
Temp. expansion coeff.	α_{f22}	K^{-1} ($^oF^{-1}$)	----------	2.3×10^{-5} (0.13×10^{-4})	----------	2.60×10^{-4} (1.55×10^{-4})
Long. compressive strength	S_{f11C}	GPa (KSI)	0.891 (130)	1.11 (161)	0.891 (130)	0.319 (134)
Long. tensile strength	S_{f11T}	GPa (KSI)	1.65 (240)	1.66 (242)	1.66 (242)	1.65 (241)
Transverse tensile strength	S_{f22T}	GPa (KSI)	0.034 (5.0)	0.038 (5.5)	0.020 (2.9)	0.023 (3.3)
Transverse compressive strength	S_{f22C}	GPa (KSI)	0.202 (29.5)	0.181 (26.4)	0.110 (16.0)	0.119 (17.3)
In-plane shear strength	S_{f12S}	GPa (KSI)	0.045 (6.6)	0.033 (4.8)	0.035 (5.1)	0.023 (3.8)
Thickness	t_f	cm (in.)	0.014 (0.0055)	0.0140 (0.00552)	----------	0.0140 (0.00552)

*From reference 8.

TABLE V. - COMPARISON OF MEASURED AND PREDICTED
ELASTIC PROPERTIES OF ANGLEPLIED LAMINATES
AS/3501-5 WITH 1.8 PERCENT MOISTURE

Laminate	Long. modulus GPa (MSI)	Trans. modulus GPa (MSI)	Shear modulus GPa (MSI)	Major Poisson's ratio
I$[O/\pm45_2/O/\pm45]_s$				
*Measured	43 (6.3)	21.2 (3.08)	22.2 (3.21)	5.54 (0.803)
Predicted	43 (6.3)	23 (3.2)	26.2 (3.80)	5.39 (0.781)
% difference	0	+3.9	+18.4	-2.70
II$[O_2/\pm45/O_2/90/O]_s$				
*Measured	89.7 (13.0)	29 (4.2)	10 (1.5)	2.24 (0.325)
Predicted	89.7 (13.0)	31 (4.5)	11 (1.6)	2.19 (0.318)
% difference	0	+7.1	+6.7	-2.2
III$[(O/\pm45/90)_2]_s$				
*Measured	46.1 (6.68)	45.7 (6.62)	16.1 (2.34)	2.42 (0.350)
Predicted	49.7 (7.20)	49.7 (7.20)	18.6 (2.70)	2.30 (0.333)
% difference	+7.8	+8.7	+15.4	-4.8

*Room temperature wet property. Measured data from reference 8.

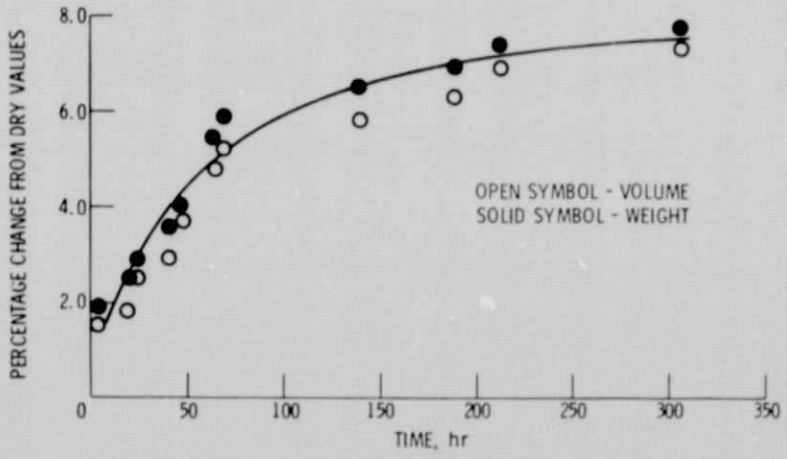

Fig. 1. - Moisture absorption characteristics of thin epoxy resin specimens in boiling water.

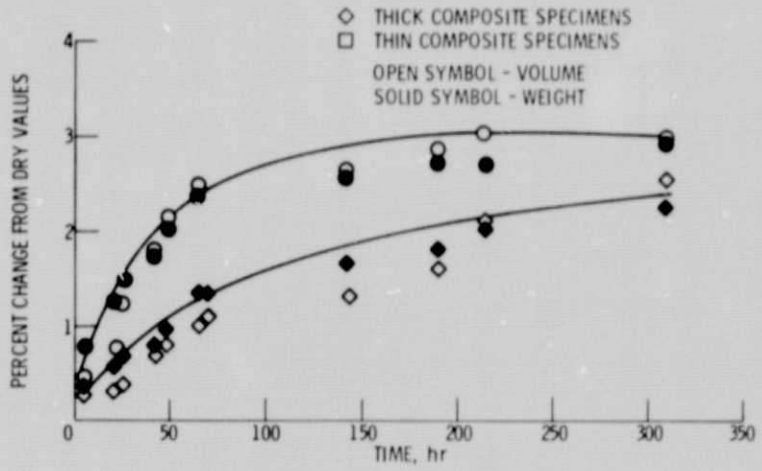

Fig. 2. - Moisture absorption characteristics of fiber/resin composite specimens in boiling water.

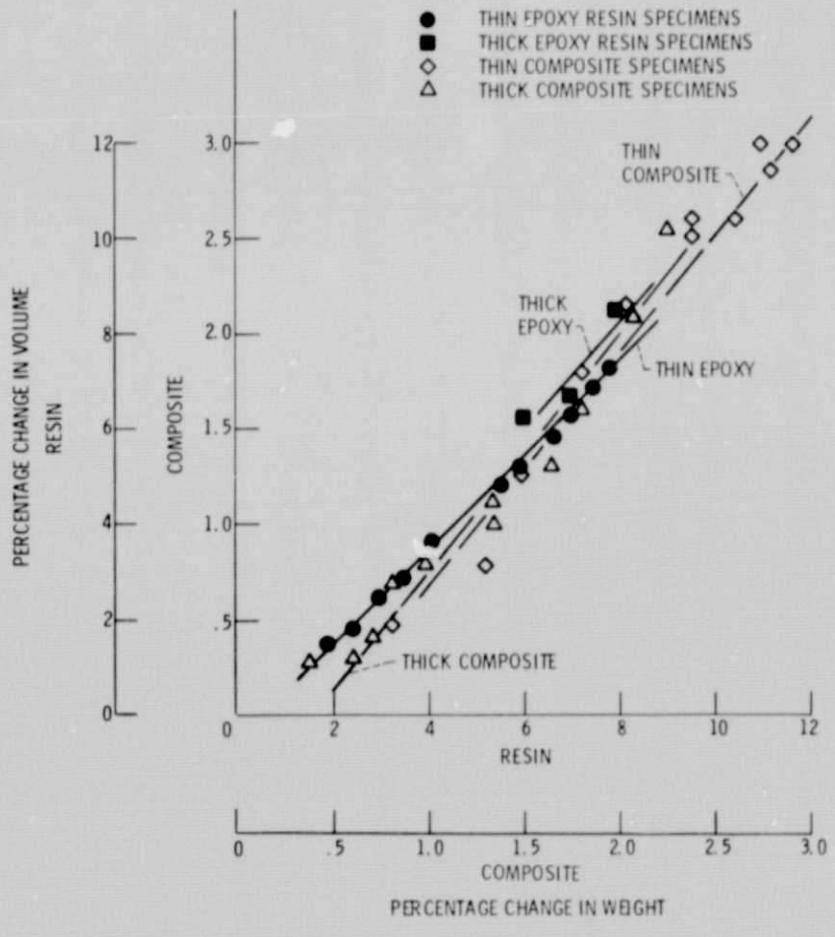

Fig. 3. - Comparison of weight and volume changes of resin and composite specimens in boiling water.

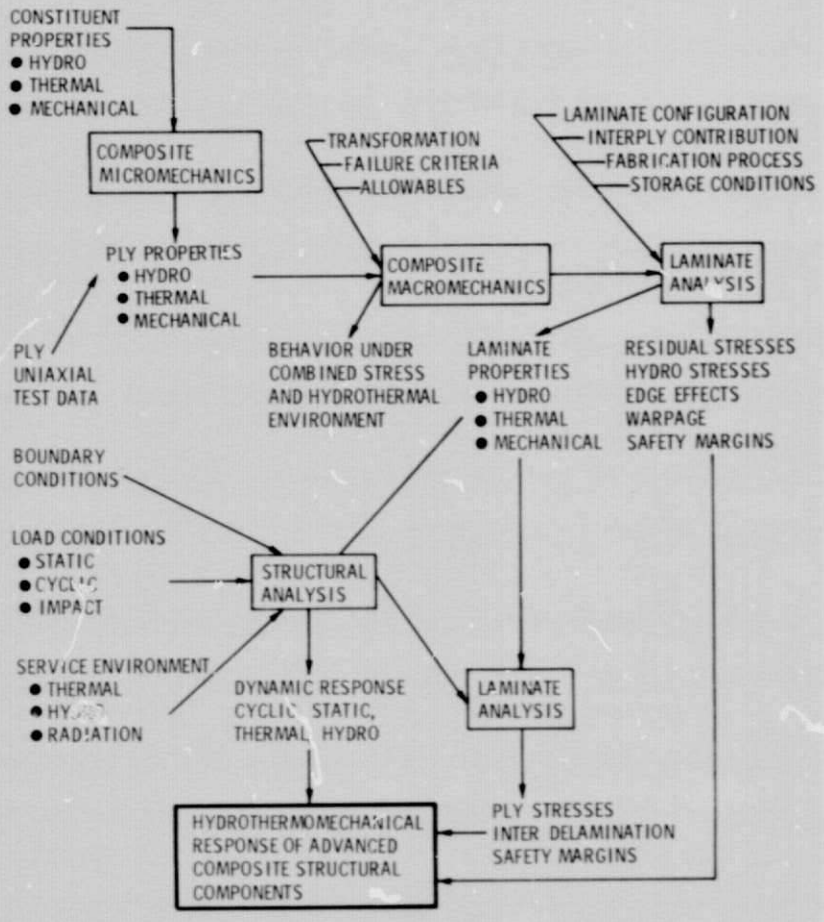

Fig. 4. - Flow diagram of integrated theory for predicting the hydrothermomechanical response of advanced composite components.

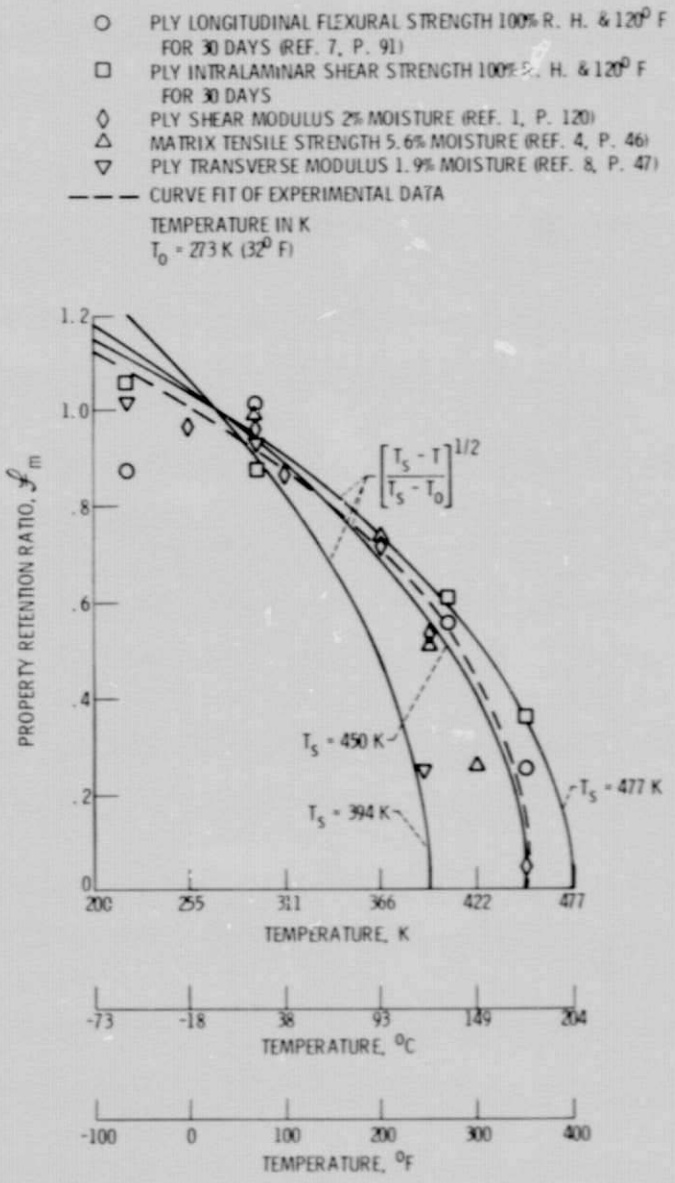

Fig. 5. - Temperature-moisture effects on composite and matrix mechanical properties (AS/3501).

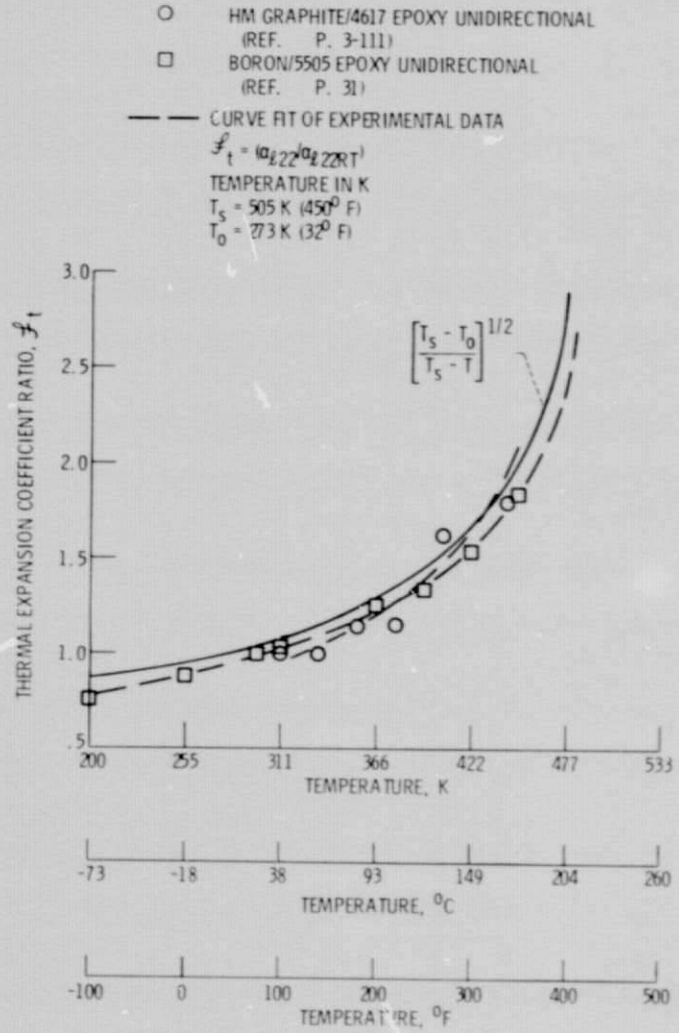

Fig. 6. - Temperature effects on thermal coefficient of expansion for unidirectional fiber/resin composites.

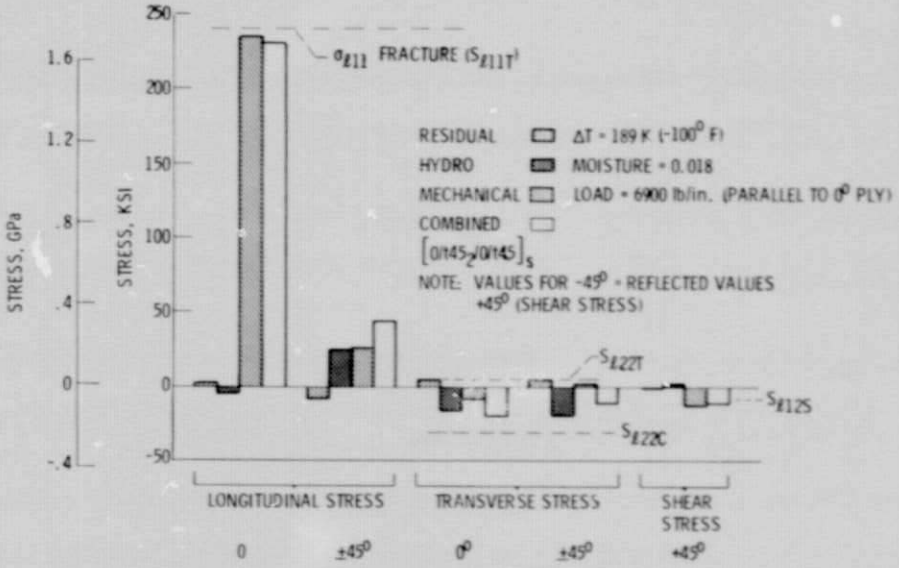

Fig. 7. - Predicted residual, hydro, mechanical and combined stresses of a multidirectional graphite-epoxy laminate.

LAMINATE ANGLES

1 - $[0/\pm45/0/\pm45]_S$

2 - $[0_2/\pm45/0_2/90/0]_S$

3 - $[(0/\pm45/90)_2]_S$

NOTE: PLY PROPERTIES FOR STRENGTH (ROOM TEMPERATURE - DRY)

PLY ELASTIC PROPERTIES (ROOM TEMPERATURE - WET)

*RANGE PREDICTED BY INTERPLY DELAMINATION

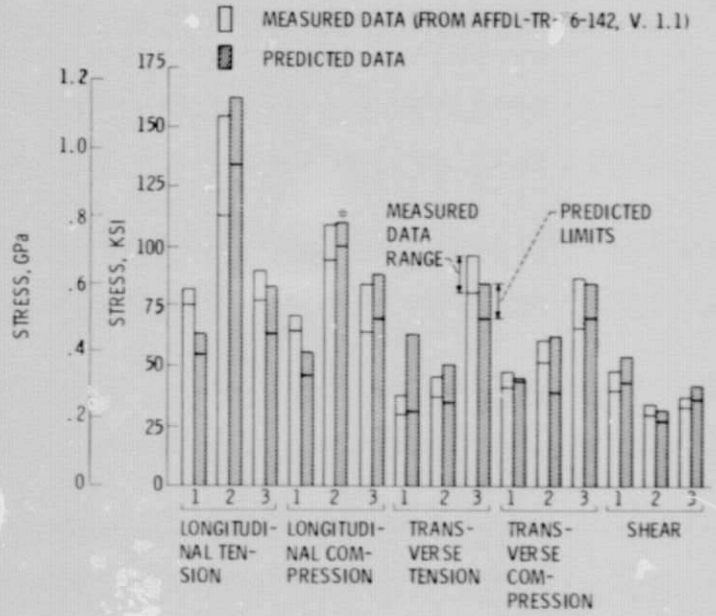

Fig. 8 - Comparison of measured and predicted fracture stresses of angle-ply laminates AS/3501-5 with 1.8% moisture.

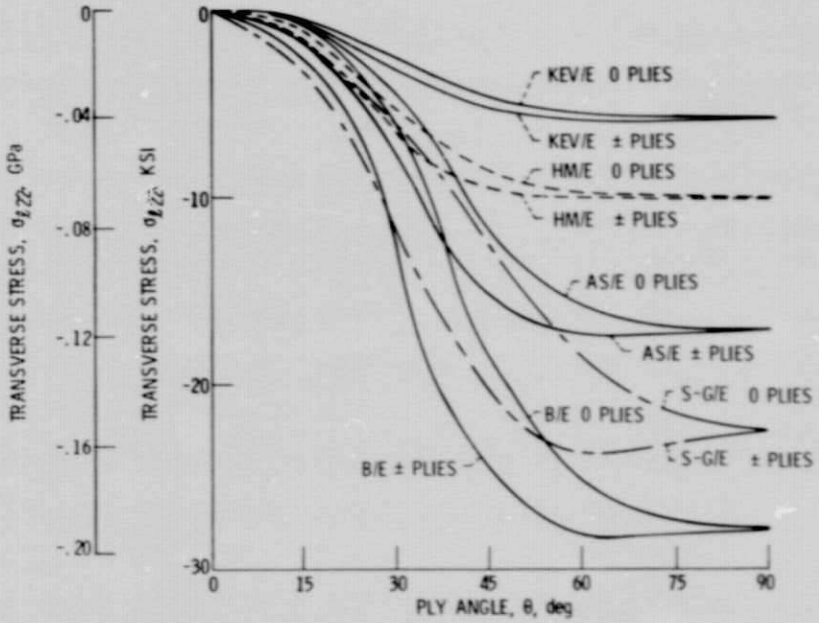

Fig. 9. - Theoretical ply transverse stresses induced by 2.5% moisture in composite system $[\theta, 0, -\theta, 0]_S$ for several materials.

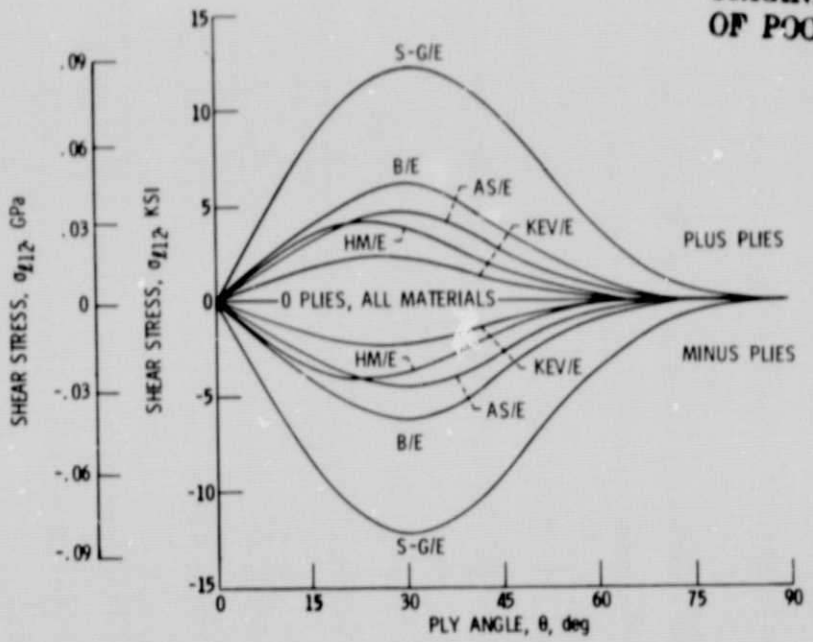

Fig. 10. - Theoretical ply shear stresses induced by 2.5% moisture in composite system $[\theta, 0, -\theta, 0]_s$ for several materials.

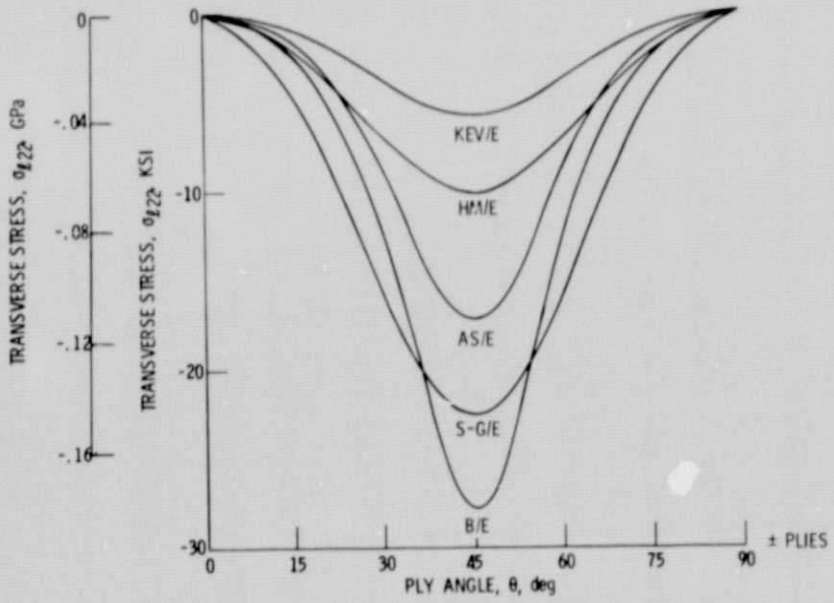

Fig. 11. - Theoretical ply transverse stresses induced by 2.5% moisture in composite system $[\theta, -\theta]_{2_s}$ for several materials.

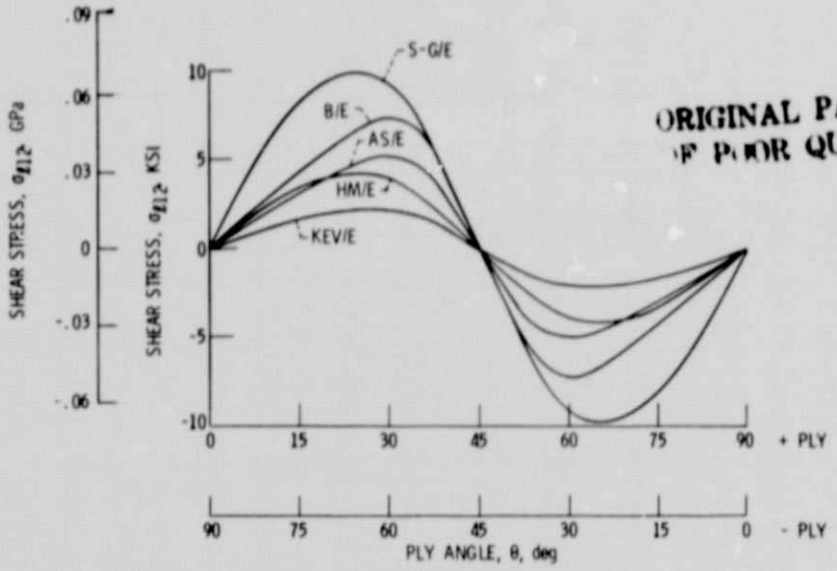

Fig. 12. - Theoretical intralaminar ply shear stresses induced by 2.5% moisture in composite system $\left[\theta, -\theta\right]_2$ for several materials.

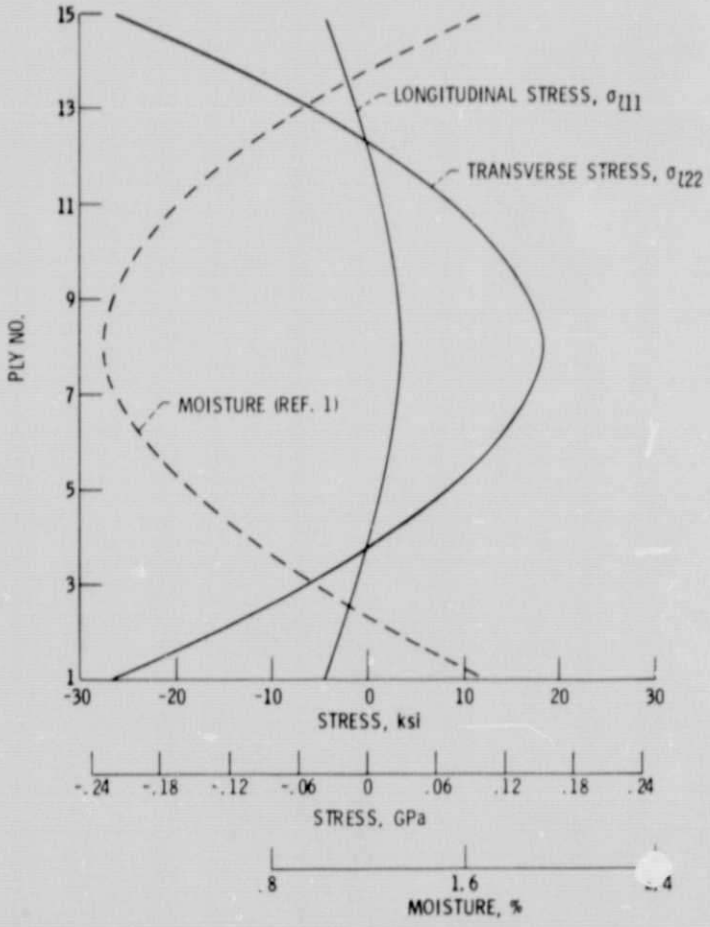

Fig. 13. - Predicted stresses induced by moisture in unidirectional boron/epoxy laminate exposed to atmosphere of 100% relative humidity for 28 days.

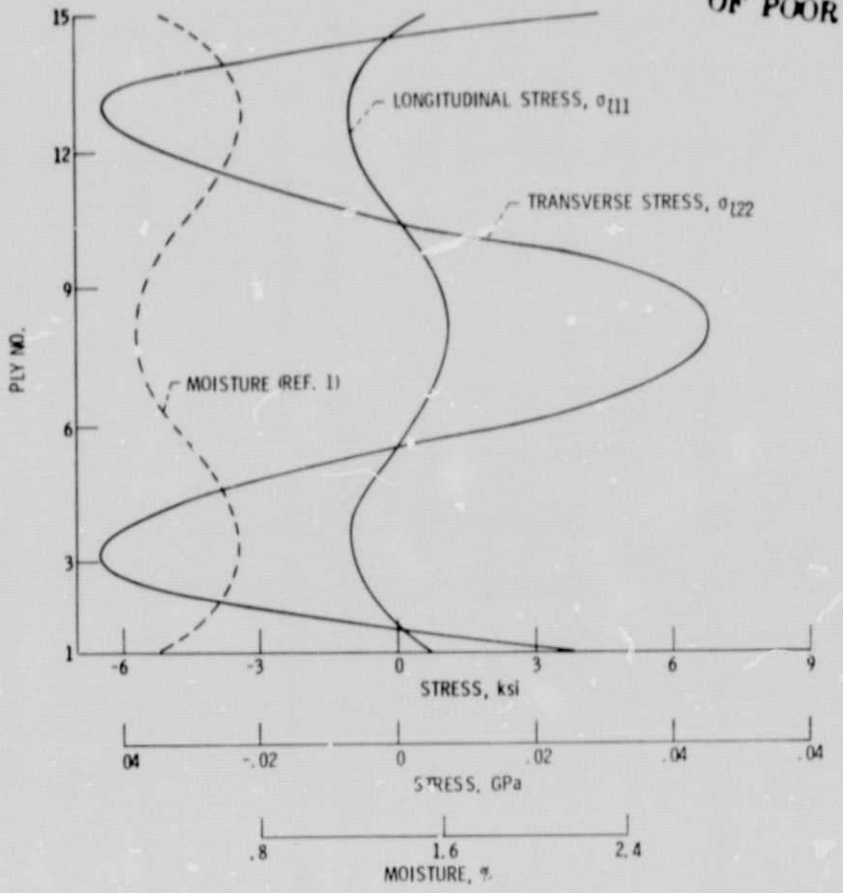

Fig. 14. - Predicted stresses induced by moisture in unidirectional boron/epoxy laminate dried 1.2 hr at 275° F.

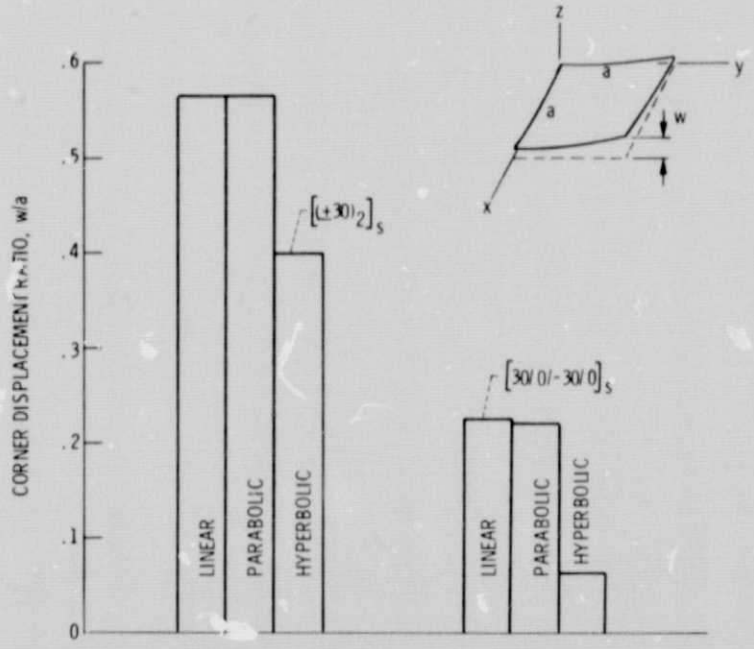

Fig. 15. - Predicted warpage induced by 2.5-percent moisture in AS/E laminates protected on one side for linear, parabolic, and hyperbolic ply moisture distributions.

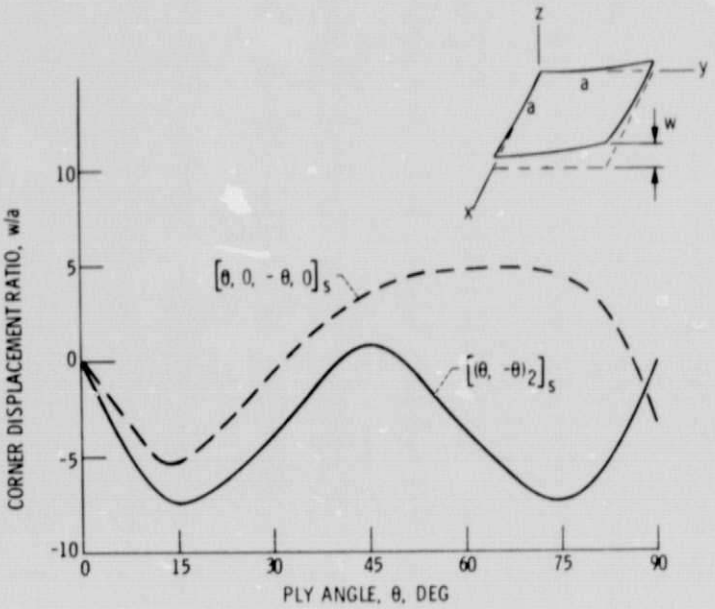

Fig. 16. - Predicted warpage induced by 2.5 percent moisture in AS/E laminates with one surface protected. (Hyperbolic moisture profile.)